

# The Kraft Break Sharply Divides Low Mass and Intermediate Mass Stars

ALEXA C. BEYER <sup>1,2</sup> AND RUSSEL J. WHITE <sup>1</sup>

<sup>1</sup>*Department of Physics and Astronomy, Georgia State University, Atlanta, GA 30303, USA*

<sup>2</sup>*Department of Physics, Astronomy, Geology and Environmental Science, Youngstown State University, Youngstown, OH 44555, USA*

## ABSTRACT

Main sequence stars transition at mid-F spectral types from slowly rotating (cooler stars) to rapidly rotating (hotter stars), a transition known as the Kraft Break (Kraft 1967) and attributed the disappearance of the outer convective envelope, causing magnetic braking to become ineffective. To define this Break more precisely, we assembled spectroscopic measurements of 405 F stars within 33.33 pc. Once young, evolved and candidate binary stars are removed, the distribution of projected rotational velocities shows the Break to be well-defined and relatively sharp. Nearly all stars redder than  $G_{BP} - G_{RP} = 0.60$  mag are slowly rotating ( $v \sin i \lesssim 20$  km/s), while only 4 of 40 stars bluer than  $G_{BP} - G_{RP} = 0.54$  mag are slowly rotating, consistent with that expected for a random distribution of inclinations. The Break is centered at an effective temperature of 6550 K and has a width of about 200 K, corresponding to a mass range of 1.32 – 1.41  $M_{\odot}$ . The Break is  $\sim 450$  K hotter than the stellar temperature at which hot Jupiters show a change in their obliquity distribution, often attributed to tidal realignment. The Break, as defined above, is nearly but not fully established in the  $\sim 650$  Myr Hyades cluster; it should be established in populations older than 1 Gyr. We propose that the Kraft Break provides a more useful division, for both professional and pedagogical purposes, between what are called low mass stars and intermediate mass stars; the Kraft Break is observationally well-defined and is linked to a change in stellar structure.

## 1. INTRODUCTION

Kraft (1967) demonstrated that nearby, non-emission line, main sequence stars exhibit a change in their rotation rates near spectral type F5. Cooler stars are slowly rotating, often with projected rotation rates below what can be measured with spectrographs (e.g.,  $v \sin i \lesssim 10$  km/s), while hotter stars rotate many times faster than this. This change in rotation had been identified in previous work (e.g., Abt & Hunter 1962; Kraft 1965), but the transition near F5 is now commonly referred to as the “Kraft Break.” Main sequence relations at the time (Iben 1967) suggested the transition occurs at a stellar mass of about 1.2  $M_{\odot}$ .

The dramatic change in rotation rate is not believed to be primordial since almost all stars over this mass range have similar rotation rates while young, at least up to about 1.6  $M_{\odot}$  (Gray 1982; Wolff & Simon 1997). Instead, the change is attributed to the effectiveness of magnetic braking. A low mass star like the Sun has an outer convective zone capable of generating a dynamo-like magnetic field (Charbonneau 2014). This field couples to the ionized stellar wind and magnetically brakes the star over time (e.g., Schatzman 1962; Weber & Davis 1967; Matt et al. 2012; Gallet & Bou-

vier 2013; van Saders et al. 2019). In contrast, a slightly higher mass star, sometimes referred to as an intermediate mass star (Aerts et al. 2019), has an outer radiative zone and is not expected to generate a magnetic field. Since these slightly higher mass stars age with no magnetic torque, they retain the angular momentum imparted during their pre-main sequence phase.

The location of the Kraft Break has provided an important reference point for understanding how the angular momentum evolution of stars relates to their internal structure (e.g., Amard et al. 2016). However, determining the precise spectral type / color / stellar mass where this Break occurs and determining how sharp the Break is has been compromised by subsets of low mass stars that remain rapidly rotating. Since magnetic braking takes 10s to 100s of millions of years to slow the rotation rate (e.g., Bouvier et al. 2014), young low mass are often rapidly rotating. Similarly, low mass short-period binary stars remain rapidly rotating if they are tidally locked to their companion (Zahn & Bouchet 1989). And finally, higher mass, post-main sequence stars that have evolved into cooler subgiant stars can be rapidly rotating (Wilson & Skumanich 1964);  $\beta$  Cassiopeiae is a well-studied example of the latter (Che et al. 2011; Zwintz et al. 2020).

Pioneering studies of stellar rotation relied mostly on spectroscopy to measure the projected rotational velocity ( $v\sin i$ ), but this provides only a lower limit on the equatorial rotational velocity. Rotationally modulated brightness variations caused by the presence of cool star spots provides a more direct way of measuring the rotation rate of a star, without the  $\sin i$  ambiguity. Photometric surveys of stars enabled by the Kepler (Borucki et al. 2010), K2 (Howell et al. 2014) and TESS (Ricker et al. 2014) missions have yielded more than 100 thousand rotation periods for low and some intermediate mass stars (e.g., Nielsen et al. 2013; McQuillan et al. 2014; Kounkel et al. 2022; Reinhold et al. 2023; Fetherolf et al. 2023; Phillips et al. 2024). These studies confirm a clear change in the rotational distribution of stars near spectral type F5<sup>1</sup>. However, because these studies include distant, less well-studied stars, the Break is blurred by populations of young, binary and evolved stars. Additionally, the disappearance of the convective zone is expected to diminish the presence of cool star spots, making it harder to measure rotation rates for stars above the Kraft Break. This is confirmed by the steep decline in the fraction of measured rotation periods with temperatures above 6000 K (e.g., McQuillan et al. 2014). Projected rotational velocity measurements (e.g.,  $v\sin i$  values) of a large sample of stars remain the least biased way to map the rotation rate of stars across the Kraft Break.

In Section 2 we use *Gaia* data to assemble a volume limited sample of F stars with  $v\sin i$  measurements. In Section 2.1 we exclude young, candidate binary and evolved stars from this sample. In Section 3 we define the location and width of the Kraft Break, and in Section 4 we investigate how well it is established in the Hyades open cluster. In Section 5 we discuss implications, including a suggestion to use the Kraft Break to more formally divide low mass stars and intermediate mass stars.

## 2. SAMPLE SELECTION AND STELLAR PROPERTY MEASUREMENTS

To identify the Kraft Break more clearly, we use *Gaia* Data Release 3 (*Gaia* DR3; *Gaia* Collaboration et al. 2016, 2023) to assemble all F stars within 33.33 pc of the Sun. Specifically, we query stars that have a parallax greater than 30 mas, a parallax uncertainty less than 1.0 mas, and have a  $G_{BP} - G_{RP}$  color between 0.327 mag (spectral type A9) and 0.784 mag (spectral type G0),

according to Pecaut & Mamajek (2013). We removed stars fainter than  $G = 10.0$  mag (190 stars) to exclude white dwarfs in this color range. The specific ADQL query used is:

```
select * from gaiadr3.gaia_source gs
where gs.parallax > 30
and gs.parallax_error < 1.0
and gs.bp_rp > 0.327
and gs.bp_rp < 0.784
and gs.phot_g_mean_mag < 10.0
```

This yields a sample of 426 stars. We note that not imposing a cut on the parallax uncertainty only increased the sample by four stars; these nearby bright stars ( $2.27 < G < 7.59$ ) have well determined parallax measurements.

Of these 426 stars, *Gaia* DR3 provides spectroscopic measures of effective temperature, surface gravity, metallicity and line broadening measurements for 349 stars (Fouesneau et al. 2023), although only 256 have *Gaia* line broadening measurements. Frémat et al. (2023) show that *Gaia*'s line broadening measurement (*vbroad*) agrees well with projected rotational velocity values ( $v\sin i$ ) over this temperature and visual brightness range. We supplement these measurements with data from the Geneva-Copenhagen survey targeting nearby F and G dwarfs (Nordström et al. 2004), and Schröder et al. (2009) targeting rapidly rotating Sun-like stars. These added 135 and 14 additional stars, respectively, for a total of 405 stars with line broadening measurements. We caution that Nordström et al. (2004) report  $v\sin i$  values as low as 0 km/s, which are likely unrealistic, and they round  $v\sin i$  values to the nearest km/s below 30 km/s, or the nearest 5 or 10 km/s above 30 km/s. The  $G_{BP} - G_{RP}$  color distributions of all 426 stars and the subset of 405 with spectroscopic measurements are shown in Figure 1.

The distance limit of 33.33 pc is chosen to avoid reddening and to maximize the fraction of stars with spectroscopic measurements and accurate stellar property assessments (Section 2.1).

To check for possible biases in the assembled measurements, we compare spectroscopic measurements from Geneva-Copenhagen with those from *Gaia* DR3 (Figure 2). Over the temperature range of 5700 K to 7000 K, a comparison of 337 temperature values shows that the Geneva-Copenhagen temperatures are on average hotter by 41 K, with the standard deviation of differences being 56 K. A comparison of 205  $v\sin i$  values shows relatively good agreement up to  $\sim 35$  km/s, with an average difference of 0.2 km/s and a standard deviation of differences of 6.1 km/s. Above 35 km/s, the measurements

<sup>1</sup> To our knowledge these studies haven't measured the Kraft Break to be at spectral type F5, but are quoting F5 as originally claimed by Kraft (1967) and reasonably consistent with their data.

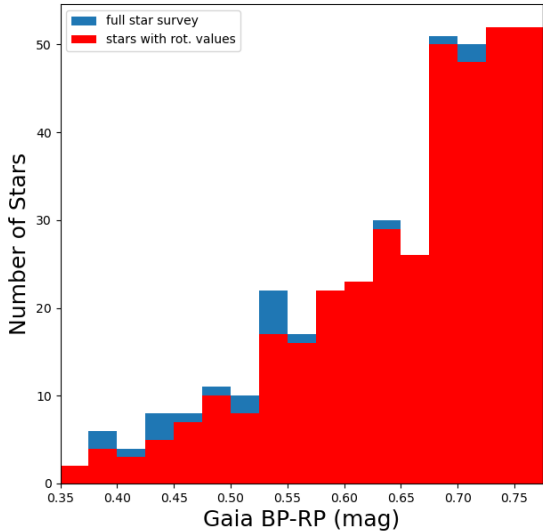


**Figure 1.** Shown is the  $G_{BP} - G_{RP}$  color distribution of 426 F stars within 33.33 pc of the Sun (*blue bars*). The subset of these with projected rotational velocity ( $v_{\text{sin}i}$ ) measurements is indicated (*red bars*).

agree less well, with an average difference of 2.0 km/s and standard deviation of differences being 19.75 km/s. However, the large dispersion is dominated by just 3 stars (see Figure 2).

### 2.1. Excluding Young, Evolved and Candidate Binary Stars

The sample of 426 F stars within 33.33 pc of the Sun is next vetted of stars that may have anomalous rotation rates, as described in Section 1. We exclude all stars that are known members of nearby Moving Groups with ages less than 200 Myr. The 12 excluded stars include the  $\beta$  Pictoris Moving Group stars HD 29391 and HD 35850, the Carina Association star HD 62848, the Columba Association star HD 29329, and the AB Dor Moving Group stars HD 17332 A, HD 25457, HD 38393, HD 45270, HD 139664, HD 141891 and HD 147584, HD 189245 (Nakajima & Morino 2012; Bell et al. 2015; Gagné et al. 2018). The stars have ages spanning from 24 Myr to 149 Myr (Bell et al. 2015) and projected rotational velocities spanning from 7 to 74 km/s. We note that the remaining sample includes 4 members of the Ursa Majoris Moving Group (HD 91480, HD 113139 A, HD 115043 and HD 116656; Gagné et al. 2018), with an estimated age of  $414 \pm 23$  Myr (Jones et al. 2015). We exclude all 117 stars flagged as known or candidate binaries in the Geneva-Copenhagen survey (Nordström et al. 2004). Although we only expect the stellar rotation to be tidally altered in short-period systems, a stellar companion may nevertheless influence a star’s rotational evolution (e.g., Patience et al. 2002; Meibom et al. 2007) and the measure of stel-

lar rotation and other stellar parameters can be biased by the presence of a spatially unresolved companion. We therefore conservatively exclude all stars flagged as such. In addition to these, we exclude stars with spectroscopically measured surface gravity values (e.g.,  $\log g$ ) less than 3.75 dex, as reported in Gaia DR3. These are suspected to be more massive stars that have evolved off the main sequence and are transitioning through the F spectral type range as subgiants. The 5 excluded stars include HD 48737, HD 68456, HD 198084, HD 219571, HD 224617; their projected rotational velocities span from 8 to 74 km/s. The sample of 405 F stars with  $v_{\text{sin}i}$  measurements, including those identified as young stars, candidate binary stars and evolved stars is illustrate in Figure 3.

## 3. DEFINING THE KRAFT BREAK

### 3.1. Color and Effective Temperature

After removing young, evolved and candidate binary stars, 295 remain in the sample. These are considered mature, single, main sequence F stars, 278 of which have  $v_{\text{sin}i}$  measurements. Figure 4 shows the distributions of projected rotation velocity ( $v_{\text{sin}i}$ ) versus Gaia  $G_{BP} - G_{RP}$  color and versus effective temperature. Both plots show an abrupt change in the distribution of  $v_{\text{sin}i}$  values at mid-F spectral types. We define the Kraft Break to be the region with a roughly uniform distribution of  $v_{\text{sin}i}$  values, above and below which the distributions are distinct as confirmed by Kolmogorov–Smirnov tests at the  $> 99.9\%$  level. In  $G_{BP} - G_{RP}$  color, the Break spans from 0.54 to 0.60. These color limits correspond closest to the  $G_{BP} - G_{RP}$  colors of an F4V star (0.546 mag) and an F5V star (0.587 mag), using the relations of Pecaut & Mamajek (2013). In Figure 4, the 217 stars redder than the Break have relatively low  $v_{\text{sin}i}$  values, with a mean value of 6.7 km/s and a standard deviation of 3.6 km/s. In contrast, the 40 stars above the Break have a mean  $v_{\text{sin}i}$  value of 63 km/s, and a standard deviation of 35 km/s. We note that only 4 out of 40 stars above the Break (10 %) have  $v_{\text{sin}i}$  values less than 30 km/s, which is consistent with that expected for a random distribution of inclinations. The results indicate that all mature, single, main sequence stars bluer than  $G_{BP} - G_{RP} = 0.54$  are rapidly rotating ( $v_{\text{sin}i} \gtrsim 20$  km/s) while those redder than  $G_{BP} - G_{RP} = 0.60$  are slowly rotating ( $v_{\text{sin}i} \lesssim 20$  km/s). This result is qualitatively consistent with the location of the Break seen in the ensemble Gaia DR3 vbroad catalog (e.g., Figure 13 in Frémat et al. 2023).

If the same criterion is used to define the Break versus effective temperature, the Break spans from 6440 – 6600 K. Adopting the color-temperature relations of Pecaut

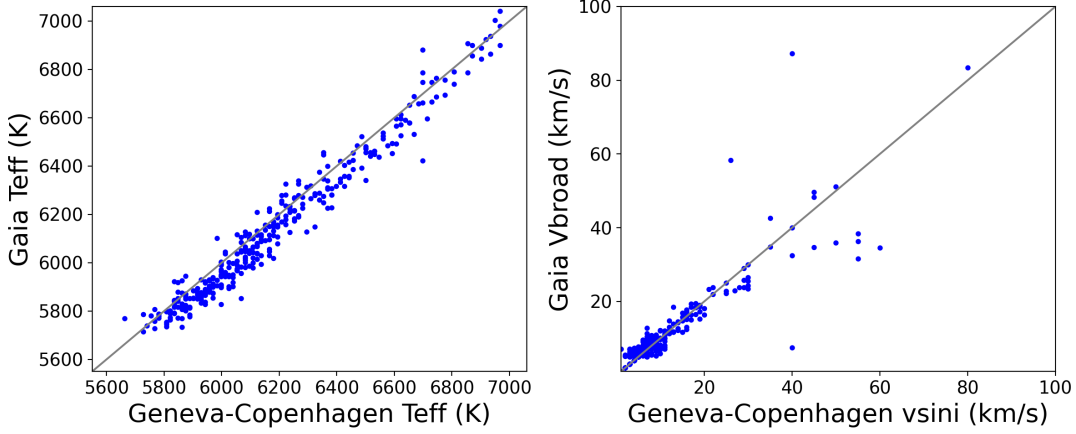


**Figure 2.** Gaia DR3 measurements of effective temperature (*left panel*) and projected rotational velocity (*right panel*) are compared with the same measurements from the Geneva-Copenhagen survey.

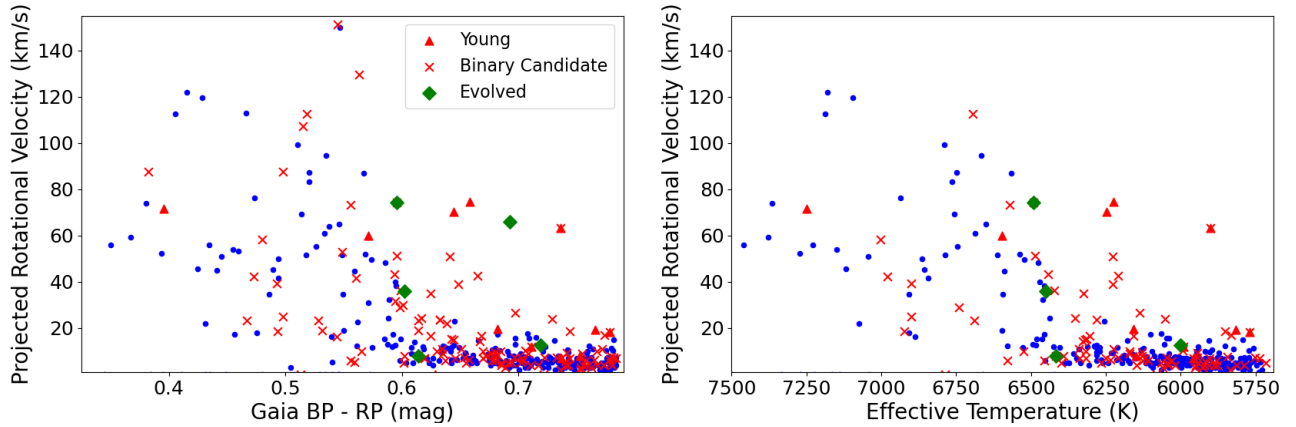


**Figure 3.** Shown are projected rotational velocities versus  $G_{BP} - G_{RP}$  color (*left panel*) and effective temperature (*right panel*). Stars identified as young, evolved or candidate binary are marked.

& Mamajek (2013), the color limits from above imply limiting temperatures of 6470 K and 6670 K, with interpolation. These limits are 30 K and 70 K hotter than those inferred from spectroscopic temperature measurements (mostly from Gaia DR3 spectra). The offset is consistent with the cooler temperatures inferred from Gaia spectra in this temperature range (41 K; Section 2). With this offset in mind and rounding to the nearest 50 K, we estimate that the Kraft Break spans from 6450 – 6650 K in temperature, with an uncertainty of  $\sim 50$  K on these limits.

In Figure 5 we illustrate the Kraft Break on an absolute  $G$  versus  $G_{BP} - G_{RP}$  diagram, plotted analogously to Figure 1 in Kraft (1967). The transition in rotation rates across the Break appears to hold over the  $\sim 2$  magnitudes vertical extent of the main sequence.

### 3.2. Stellar Mass and Metallicity

We estimate the stellar mass limits of measured Kraft Break using components of eclipsing binaries from Tor-

res et al. (2010). We restrict the comparison sample to those with masses between  $1.05 M_{\odot}$  and  $1.60 M_{\odot}$ ; these stars have an average mass uncertainty of 0.8% and an average temperature uncertainty of 1.9%. From the sample of 59 stars within this mass range, we exclude 6 stars with  $\log g$  values below 4.0 dex as suspected of being evolved. Using the Kraft Break temperature edges of 6450 K and 6650 K, a linear fit to the mass versus temperature distribution of these eclipsing binary stars yields mass edges of  $1.32 M_{\odot}$  and  $1.41 M_{\odot}$  (Figure 6). We approximate a  $1\sigma$  uncertainty by varying the y-intercept by  $\pm 160$  K to include 2/3rd of the data. This suggests the mass limits of the Break are uncertain by  $0.07 M_{\odot}$ . These values are in good agreement using the color / temperature / mass relations from Pecaut & Mamajek (2013); the  $G_{BP} - G_{RP}$  color edges of the Break correspond to masses of  $1.31 M_{\odot}$  and  $1.39 M_{\odot}$ , and the effective temperature edges of the Break correspond to  $1.30 M_{\odot}$  and  $1.39 M_{\odot}$ . We therefore adopt

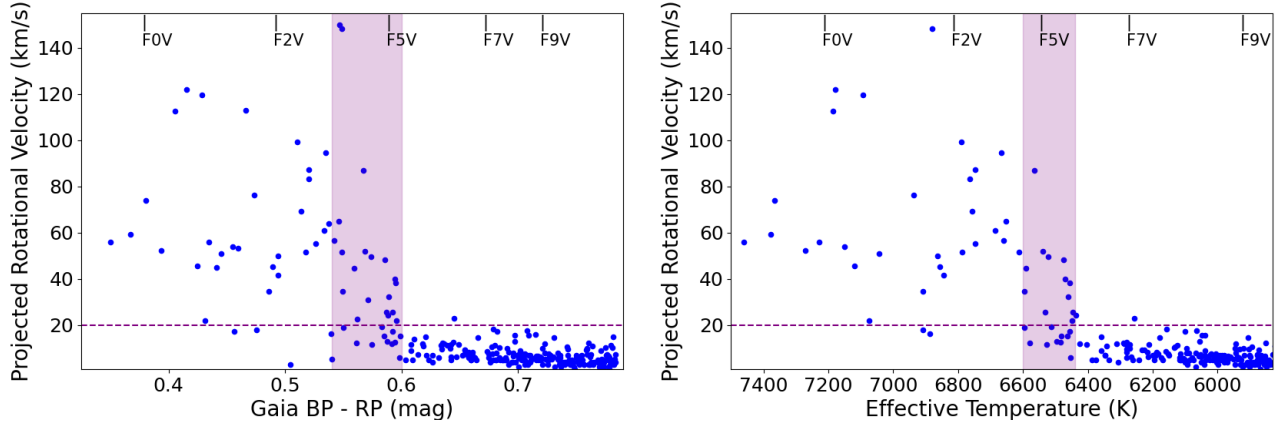


**Figure 4.** Shown are the projected rotational velocities versus  $G_{BP} - G_{RP}$  color (*left panel*) and effective temperature (*right panel*) after removing young, evolved and candidate binary stars. The roughly uniform distributions of  $v \sin i$  values in the shaded regions are used to define the location and width of the Kraft Break (see Section 3).

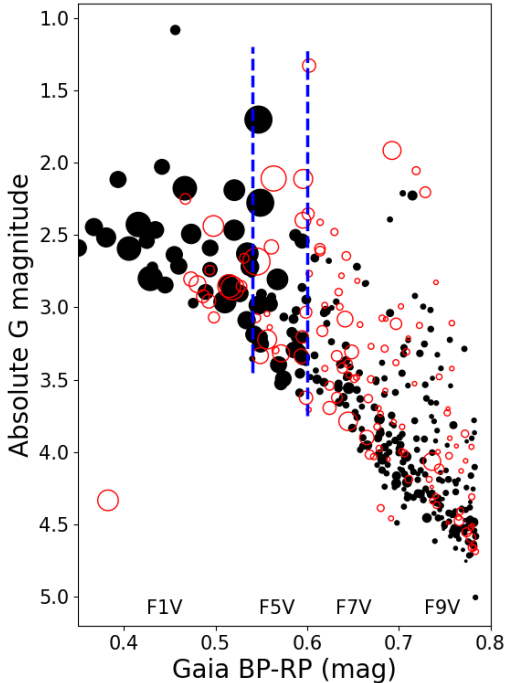


**Figure 5.** The 33.33 pc sample of F stars is plotted on an absolute  $G$  versus  $G_{BP} - G_{RP}$  diagram. Young, evolved and candidate binary stars (*open circles*) are distinguished from those that are not (*filled circles*), as described in Section 2.1. Circle sizes are scaled by the projected rotational velocity ( $v \sin i$ ) values. The dashed vertical lines mark the color boundaries of the Kraft Break. The anomalous outlier at the lower left of the plot is HD 194943 B; its photometry may be biased by its brighter  $1''.64$  companion (Makarov & Fabricius 2021).

the mass edges from the eclipsing binary analysis and estimate that the Kraft Break spans from  $1.32 M_{\odot}$  to  $1.41 M_{\odot}$  in mass.

Metallicity affects the opacity within the outer, partial ionization zones and thus can alter both the depth of convection and convective turnover time. These changes in turn affect the efficiency of magnetic braking, with the general trend that metal-rich stars spin down more effectively than metal-poor stars (e.g., van Saders et al. 2019; Amard & Matt 2020). The location of the Kraft Break in color / temperature / mass may therefore be metallicity dependent, but the 33.33 pc F star sample studied here does not show any evidence of this. The Kraft Break is located within the same temperature / color range for subsamples of stars above and below the median metallicity ( $[Fe/H] = -0.43$  dex); both subsamples span the full width of the Break. We caution however that the sample is too small to investigate the effect of metallicity accurately, in part because the first-release metallicity values from Gaia are considered to be biased (Reinhold et al. 2023); the median value is low compared to values measured in detailed spectroscopic studies of F stars (e.g., Reddy et al. 2003).

#### 4. THE KRAFT BREAK IN THE HYADES OPEN CLUSTER

The above results indicate that after a few hundred million years, single, main sequence stars cooler than  $\sim 6450$  K will be slowly rotating. As a first check of when the Break is established, we conduct a similar analysis of F stars in the well studied, nearby ( $46.75 \pm 0.46$  pc; Gaia Collaboration et al. 2017), Hyades open cluster, with an age of  $650 \pm 50$  Myr (Perryman et al. 1998; Martín et al. 2018; Gossage et al. 2018). Hyades members are selected from Brandner et al. (2023) and are restricted to those identified as single and within the same  $G_{BP} - G_{RP}$  color range (0.327 - 0.784 mag). This yielded 50 stars, 42 of which have color,  $v \sin i$  and effective temperature measurements from Gaia DR3. We note that the av-



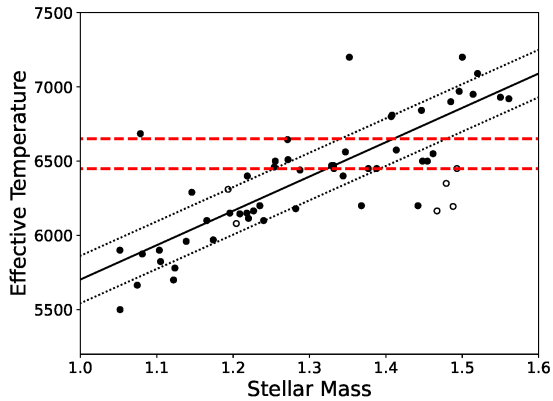


**Figure 6.** Effective temperature versus stellar mass for components of eclipsing binaries from [Torres et al. \(2010\)](#). The temperature limits of the Kraft Break are shown as *dashed lines*. A linear fit to the eclipsing binary data is used to define the corresponding mass limits of the Kraft Break (*solid line*) and uncertainties (*dotted lines*). Components with  $\log g < 4.0$  dex (*open circles*) are excluded from the fit.

erage reddening for stars in the Hyades is measured to be small, but possibly non-zero ( $E(B-V) \leq 0.001$  mag; [Taylor 2006](#)); we make no reddening corrections to their colors.

Figure 7 shows the projected rotational distributions of these 42 Hyads versus  $G_{BP} - G_{RP}$  color and effective temperature. The Break regions identified for the 33.33 pc sample are over-plotted for comparison. The distributions show a similar pattern, consistent with the initial investigation by [Kraft \(1965\)](#). Stars hotter than the Break are consistent with a randomly oriented, rapidly rotating sample, stars within the Break region have an intermediate spread in  $v \sin i$  values, and most of the stars cooler than the Break are slowly rotating ( $v \sin i < 20$  km/s). The primary difference is that a few stars close to but just redder / cooler than the Break have modest rotation. Two stars that have colors redder than the Break region are identified as rapidly rotating (with  $G_{BP} - G_{RP}$  colors of 0.602 and 0.624 and  $v \sin i$  values of 33.0 km/s and 26.1 km/s, respectively). Five stars that have temperatures cooler than the Break region are identified as rapidly rotating (with temperatures spanning 6282 K to 6436 K, and  $v \sin i$  values spanning 26.1 km/s - 33.0 km/s). We speculate that these mid-F stars have not had time to slow sufficiently and establish the Kraft Break as defined here. Given these results along with evidence of how rotation declines with age for stars less massive than the Break (e.g., [Gallet & Bouvier 2013](#); [van Saders et al. 2019](#); [Curtis et al. 2020](#); [Clayton et al. 2020](#); [Godoy-Rivera et al. 2021](#)), we speculate that the Break should be fully established by these criterion by 1 Gyr.

## 5. DISCUSSION AND CONCLUSIONS

The above analysis shows that the Kraft Break is well-defined, occurring at a central effective temperature of  $\sim 6550$  K, central  $G_{BP} - G_{RP}$  color of  $\sim 0.57$  mag, and central mass of  $1.37 M_{\odot}$ . The Break is relatively sharp, having a width of only 200 K in temperature,  $\sim 0.06$  mag in color and  $\sim 0.11 M_{\odot}$  in mass. We note that these values are all larger than measurement uncertainties; the Break has width. The location of the Kraft Break is consistent with both theoretical (e.g., Figure 6 in [van Saders & Pinsonneault 2013](#)) and observational (e.g., [Godoy-Rivera et al. 2021](#)) values of the effective temperature and stellar mass at which stars exhibit a marked change in their rotational evolution, but it is now more sharply defined. This mass is consistent with the mass at which stars transition from having a thick convective envelope to having thin, separate convective layers stemming from H and He ionization ([Cantiello & Braithwaite 2019](#); [Jermyn et al. 2022](#)). And this temperature closely matches the temperature at which stars exhibit a dramatic shift in average surface gravity values (e.g., Figure 7 in [Avallone et al. 2022](#)), confirming a bona-fide change in structure. Here we discuss some implications.

### 5.1. Implications for Population Studies of Stars

With very few exceptions, stars cooler than the Kraft Break that are rapidly rotating are either young ( $< 1$  Gyr), candidate binary stars or evolved sub-giants. Rotation thus provides a blunt tracer for evolution or binarity in this mass regime, as is generally known (e.g., [Rampalli et al. 2023](#)). Correspondingly, stars hotter than the Kraft Break with low  $v \sin i$  values are likely pole-on rapid rotators (e.g., Vega; [Aufdenberg et al. 2006](#)). This has implications for RV planet searches that target low  $v \sin i$  subsets of Sun-like stars to optimize RV precision (e.g., [Quinn et al. 2012](#); [Lagrange et al. 2013](#)). Assuming a low obliquity, planetary companions orbiting low  $v \sin i$  early-F stars will have reduced RV amplitudes (by  $\sin i$ ) and will likely not transit.

Very rapidly rotating stars, those with equatorial velocities  $\gtrsim 100$  km/s, with nearly pole-on orientations will also have biased apparent colors, effective temperatures and luminosities because of their oblate shape and gravity darkening ([Owocki et al. 1994](#); [van Belle 2012](#)). As an example, [Che et al. \(2011\)](#) show, based on interferometric imaging, that the nearly pole-on orientation of the F2 star  $\beta$  Cassiopeiae appears  $\sim 400$  K hotter and  $\sim 55\%$  more luminous than if viewed edge-on. This will translate to a spread in the single-star main sequence for stars more massive than the Kraft Break. If unrecognized, nearly pole-on rapid rotators

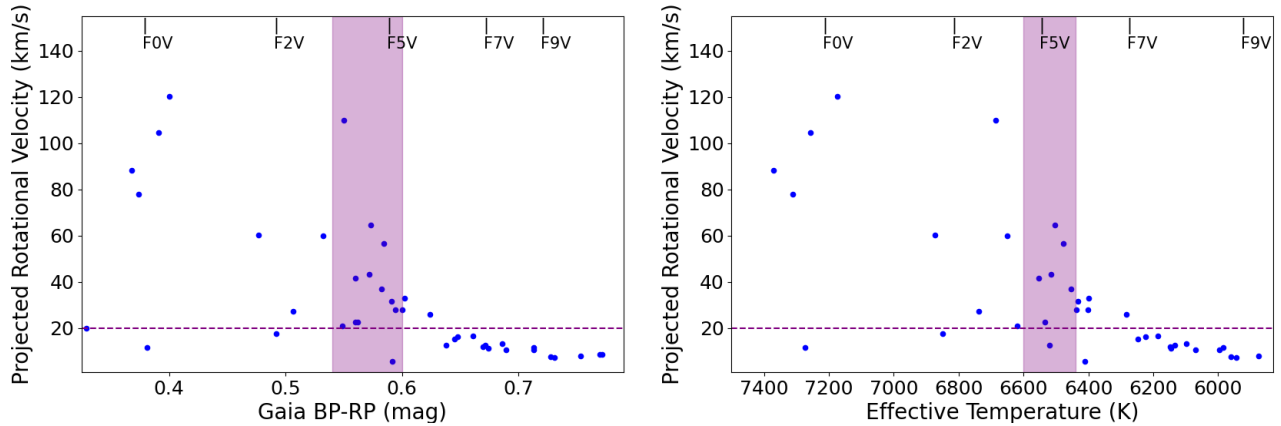


**Figure 7.** Shown are the projected rotational velocities versus  $G_{BP} - G_{RP}$  colors (*left panel*) and effective temperatures (*right panel*) of 49 single F stars in the Hyades. The shaded regions define the location and width of the Kraft Break as determined from the 33.33 pc F star sample in Figure 4.

could be misclassified as photometric binaries, biasing comparisons with evolutionary models (e.g., Brandner et al. 2023). This effect will also complicate age estimates that rely on a single main-sequence turnoff point. This is a known problem for nearby open clusters (e.g., Hyades, Praesepe, Ursa Majoris; Brandt & Huang 2015; Jones et al. 2015; Gossage et al. 2019), but it is likely a problem for any cluster younger than  $\sim 3$  Gyr, the approximate main sequence lifetime of stars within the Kraft Break.

### 5.2. Implications for Exoplanet Obliquities

Albrecht et al. (2022), Spalding & Winn (2022) and others have shown that hot Jupiters orbiting cool stars tend to have low obliquities while those orbiting hotter stars have a broad range of obliquities, consistent with random inclinations. These population studies estimate a transition in the obliquity distribution at  $\sim 6100$  K, corresponding to  $1.17 \pm 0.07 M_{\odot}$  from the temperature / mass relation of Figure 6; estimates from original work span from 6000 K to 6250 K, however (e.g., Schlaufman 2010; Winn et al. 2010). A favored interpretation for the transition is that the slower rotation and different internal structure of cooler stars may enhance tidal realignment of the outer atmospheres of stars (Dawson 2014; Rice et al. 2022). These cooler mass stars may have had a similar, random distribution of obliquities initially, but for these stars tides induced by the planet realigns the outer atmosphere of the star to rotate in the plane of its orbit. This transition in the obliquity distribution is often stated as occurring at the Kraft Break (e.g., Rice et al. 2022; Wright et al. 2023), but the results here suggest that it occurs some 450 K cooler than the Kraft Break. The basic interpretation of tidal realignment may nevertheless be correct. Considering these phenomenon as a function of increasing stellar mass and

effective temperatures, tidal realignment appears to become ineffective before magnetic braking becomes ineffective.

### 5.3. A Better Division Between Low Mass and Intermediate Mass Stars

For both professional and pedagogical purposes, it is well accepted that “high mass stars” are those that end their life in a iron-core collapse supernova. Theoretical and observational studies find that this occurs for stars more massive than  $\sim 7 - 9 M_{\odot}$  (see discussion in Cinquegrana et al. 2023), with  $8 M_{\odot}$  being a common approximate value. Lower mass stars, those that end their life as a white dwarf, are similarly often divided into low mass stars and intermediate mass stars, although the division between these is less well-defined.

The most formal division between low mass stars and intermediate mass stars stems from historical theoretical work. Iben (1967) first identified that stars more massive than  $2.25 M_{\odot}$ , according to their calculations, do not experience a helium flash; the helium cores of more massive stars are ignited during post-main sequence evolution in a non-degenerate state. Many stellar structure and evolution textbooks now define this as a division between low mass and intermediate mass stars (e.g., Lamers & Levesque 2017). And introductory astronomy textbooks adopt a similar division, rounded to “about 2 solar masses” (e.g., Bennett et al. 2004). Separating stars by mass provides a way to discuss the differences in structure, changes in dominant fusion processes and rates of evolution between Sun-like stars and those more massive than the Sun, even though they all end their life as white dwarfs. But the specific reason for the division between low mass and intermediate mass stars is usually not discussed at the introductory level, possibly because it’s too subtle to be relevant at this level. But

classroom experience confirms that this omission, in contrast to the well-defined division between intermediate mass and high mass stars, raises questions from astute students.

The ‘post-main sequence, non-degenerate core’ division between low mass stars and intermediate mass stars is not widely used by the scientific community, however. In some cases “intermediate mass” appears to be used to simply distinguish a subsample of stars with larger or smaller masses, but in many cases this division appears to be prompted by the different stellar properties associated with stars above and below the Kraft Break (e.g., Carlberg 2014; Pouilly et al. 2020; Nguyen et al. 2022; Pereira et al. 2024; Johnston et al. 2024).

We propose that the Kraft Break provides a less ambiguous and a more useful division between low and intermediate mass stars. The Break is observationally well-defined, providing a clear distinction for main sequence stars. The Break is physically linked to a change in stellar structure, the disappearance of the outer convective envelope. This change in structure is already the adopted transition point to “intermediate mass star” in some review studies (e.g. Aerts et al. 2019). This division could be related to topics that are discussed more thoroughly in both introductory and graduate-level astronomy textbooks - the presence of an outer convective zone. And fortuitously the Kraft Break occurs close to two other important stellar transition points - the onset

of core convection caused by the CNO-cycle dominating energy production (Kippenhahn & Weigert 1990) and the red-edge of the instability strip (Kaye et al. 1999; Kurtz 2022). For all of these reasons, we propose that the Kraft Break provides a more useful division, for both pedagogical and scientific purposes, between what are classified as low mass stars and intermediate mass stars.

We would like to thank Colin Kane, Becky Flores, Todd Henry and John Meftah for helpful discussions, and we extend a special thanks to Wei-Chun Jao, Jeremy Jones and Zachary Way for critically reading a first draft. We thank Jamie Tayar for noting the alignment of the Kraft Break with the global shift in stellar surface gravity values. This research was supported by National Science Foundation grant No. 2050829 to Georgia State University under the Research Experiences for Undergraduates program. This research has made use of the SIMBAD database, operated at CDS, Strasbourg, France. This work has made use of data from the European Space Agency (ESA) mission *Gaia* (<https://www.cosmos.esa.int/gaia>), processed by the *Gaia* Data Processing and Analysis Consortium (DPAC, <https://www.cosmos.esa.int/web/gaia/dpac/consortium>). Funding for the DPAC has been provided by national institutions, in particular the institutions participating in the *Gaia* Multilateral Agreement. This research has made use of NASA’s Astrophysics Data System.

## REFERENCES

- Abt, H. A., & Hunter, James H., J. 1962, *ApJ*, 136, 381, doi: [10.1086/147391](https://doi.org/10.1086/147391)
- Aerts, C., Mathis, S., & Rogers, T. M. 2019, *ARA&A*, 57, 35, doi: [10.1146/annurev-astro-091918-104359](https://doi.org/10.1146/annurev-astro-091918-104359)
- Albrecht, S. H., Dawson, R. I., & Winn, J. N. 2022, *PASP*, 134, 082001, doi: [10.1088/1538-3873/ac6c09](https://doi.org/10.1088/1538-3873/ac6c09)
- Amard, L., & Matt, S. P. 2020, *ApJ*, 889, 108, doi: [10.3847/1538-4357/ab6173](https://doi.org/10.3847/1538-4357/ab6173)
- Amard, L., Palacios, A., Charbonnel, C., Gallet, F., & Bouvier, J. 2016, *A&A*, 587, A105, doi: [10.1051/0004-6361/201527349](https://doi.org/10.1051/0004-6361/201527349)
- Auffenberg, J. P., Mérand, A., Coudé du Foresto, V., et al. 2006, *ApJ*, 645, 664, doi: [10.1086/504149](https://doi.org/10.1086/504149)
- Avallone, E. A., Tayar, J. N., van Saders, J. L., et al. 2022, *ApJ*, 930, 7, doi: [10.3847/1538-4357/ac60a1](https://doi.org/10.3847/1538-4357/ac60a1)
- Bell, C. P. M., Mamajek, E. E., & Naylor, T. 2015, *MNRAS*, 454, 593, doi: [10.1093/mnras/stv1981](https://doi.org/10.1093/mnras/stv1981)
- Bennett, J. O., Donahue, M., Schneider, N., & Voit, M. 2004, *The Cosmic Perspective*
- Borucki, W. J., Koch, D., Basri, G., et al. 2010, *Science*, 327, 977, doi: [10.1126/science.1185402](https://doi.org/10.1126/science.1185402)
- Bouvier, J., Matt, S. P., Mohanty, S., et al. 2014, in *Protostars and Planets VI*, ed. H. Beuther, R. S. Klessen, C. P. Dullemond, & T. Henning, 433–450, doi: [10.2458/azu\\_uapress.9780816531240-ch019](https://doi.org/10.2458/azu_uapress.9780816531240-ch019)
- Brandner, W., Calissendorff, P., & Kopytova, T. 2023, *MNRAS*, 518, 662, doi: [10.1093/mnras/stac2247](https://doi.org/10.1093/mnras/stac2247)
- Brandt, T. D., & Huang, C. X. 2015, *ApJ*, 807, 58, doi: [10.1088/0004-637X/807/1/58](https://doi.org/10.1088/0004-637X/807/1/58)
- Cantiello, M., & Braithwaite, J. 2019, *ApJ*, 883, 106, doi: [10.3847/1538-4357/ab3924](https://doi.org/10.3847/1538-4357/ab3924)
- Carlberg, J. K. 2014, *AJ*, 147, 138, doi: [10.1088/0004-6256/147/6/138](https://doi.org/10.1088/0004-6256/147/6/138)
- Charbonneau, P. 2014, *ARA&A*, 52, 251, doi: [10.1146/annurev-astro-081913-040012](https://doi.org/10.1146/annurev-astro-081913-040012)
- Che, X., Monnier, J. D., Zhao, M., et al. 2011, *ApJ*, 732, 68, doi: [10.1088/0004-637X/732/2/68](https://doi.org/10.1088/0004-637X/732/2/68)
- Cinquegrana, G. C., Joyce, M., & Karakas, A. I. 2023, *MNRAS*, 525, 3216, doi: [10.1093/mnras/stad2461](https://doi.org/10.1093/mnras/stad2461)



- Claytor, Z. R., van Saders, J. L., Santos, Â. R. G., et al. 2020, *ApJ*, 888, 43, doi: [10.3847/1538-4357/ab5c24](https://doi.org/10.3847/1538-4357/ab5c24)
- Curtis, J. L., Agüeros, M. A., Matt, S. P., et al. 2020, *ApJ*, 904, 140, doi: [10.3847/1538-4357/ab5f58](https://doi.org/10.3847/1538-4357/ab5f58)
- Dawson, R. I. 2014, *ApJL*, 790, L31, doi: [10.1088/2041-8205/790/2/L31](https://doi.org/10.1088/2041-8205/790/2/L31)
- Fetherolf, T., Pepper, J., Simpson, E., et al. 2023, *ApJS*, 268, 4, doi: [10.3847/1538-4365/acdee5](https://doi.org/10.3847/1538-4365/acdee5)
- Fouesneau, M., Frémat, Y., Andrae, R., et al. 2023, *A&A*, 674, A28, doi: [10.1051/0004-6361/202243919](https://doi.org/10.1051/0004-6361/202243919)
- Frémat, Y., Royer, F., Marchal, O., et al. 2023, *A&A*, 674, A8, doi: [10.1051/0004-6361/202243809](https://doi.org/10.1051/0004-6361/202243809)
- Gagné, J., Roy-Loubier, O., Faherty, J. K., Doyon, R., & Malo, L. 2018, *ApJ*, 860, 43, doi: [10.3847/1538-4357/aac2b8](https://doi.org/10.3847/1538-4357/aac2b8)
- Gaia Collaboration, Prusti, T., de Bruijne, J. H. J., et al. 2016, *A&A*, 595, A1, doi: [10.1051/0004-6361/201629272](https://doi.org/10.1051/0004-6361/201629272)
- Gaia Collaboration, van Leeuwen F., Vallenari, A., et al. 2017, *VizieR Online Data Catalog*, J/A+A/601/A19, doi: [10.26093/cds/vizieer.36010019](https://doi.org/10.26093/cds/vizieer.36010019)
- Gaia Collaboration, Vallenari, A., Brown, A. G. A., et al. 2023, *A&A*, 674, A1, doi: [10.1051/0004-6361/202243940](https://doi.org/10.1051/0004-6361/202243940)
- Gallet, F., & Bouvier, J. 2013, *A&A*, 556, A36, doi: [10.1051/0004-6361/201321302](https://doi.org/10.1051/0004-6361/201321302)
- Godoy-Rivera, D., Pinsonneault, M. H., & Rebull, L. M. 2021, *ApJS*, 257, 46, doi: [10.3847/1538-4365/ac2058](https://doi.org/10.3847/1538-4365/ac2058)
- Gossage, S., Conroy, C., Dotter, A., et al. 2018, *ApJ*, 863, 67, doi: [10.3847/1538-4357/aad0a0](https://doi.org/10.3847/1538-4357/aad0a0)
- . 2019, *ApJ*, 887, 199, doi: [10.3847/1538-4357/ab5717](https://doi.org/10.3847/1538-4357/ab5717)
- Gray, D. F. 1982, *ApJ*, 261, 259, doi: [10.1086/160336](https://doi.org/10.1086/160336)
- Howell, S. B., Sobek, C., Haas, M., et al. 2014, *PASP*, 126, 398, doi: [10.1086/676406](https://doi.org/10.1086/676406)
- Iben, Icko, J. 1967, *ApJ*, 147, 650, doi: [10.1086/149041](https://doi.org/10.1086/149041)
- Jermyn, A. S., Anders, E. H., Lecoanet, D., & Cantiello, M. 2022, *ApJS*, 262, 19, doi: [10.3847/1538-4365/ac7cee](https://doi.org/10.3847/1538-4365/ac7cee)
- Johnston, H. F., Panić, O., & Liu, B. 2024, *MNRAS*, 527, 2303, doi: [10.1093/mnras/stad3254](https://doi.org/10.1093/mnras/stad3254)
- Jones, J., White, R. J., Boyajian, T., et al. 2015, *ApJ*, 813, 58, doi: [10.1088/0004-637X/813/1/58](https://doi.org/10.1088/0004-637X/813/1/58)
- Kaye, A. B., Handler, G., Krisciunas, K., Poretti, E., & Zerbi, F. M. 1999, *PASP*, 111, 840, doi: [10.1086/316399](https://doi.org/10.1086/316399)
- Kippenhahn, R., & Weigert, A. 1990, *Stellar Structure and Evolution*
- Kounkel, M., Stassun, K. G., Bouma, L. G., et al. 2022, *AJ*, 164, 137, doi: [10.3847/1538-3881/ac866d](https://doi.org/10.3847/1538-3881/ac866d)
- Kraft, R. P. 1965, *ApJ*, 142, 681, doi: [10.1086/148330](https://doi.org/10.1086/148330)
- . 1967, *ApJ*, 150, 551, doi: [10.1086/149359](https://doi.org/10.1086/149359)
- Kurtz, D. W. 2022, *ARA&A*, 60, 31, doi: [10.1146/annurev-astro-052920-094232](https://doi.org/10.1146/annurev-astro-052920-094232)
- Lagrange, A. M., Meunier, N., Chauvin, G., et al. 2013, *A&A*, 559, A83, doi: [10.1051/0004-6361/201220770](https://doi.org/10.1051/0004-6361/201220770)
- Lamers, H. J. G. L. M., & Levesque, E. M. 2017, *Understanding Stellar Evolution*, doi: [10.1088/978-0-7503-1278-3](https://doi.org/10.1088/978-0-7503-1278-3)
- Makarov, V. V., & Fabricius, C. 2021, *AJ*, 162, 260, doi: [10.3847/1538-3881/ac2ee0](https://doi.org/10.3847/1538-3881/ac2ee0)
- Martín, E. L., Lodieu, N., Pavlenko, Y., & Béjar, V. J. S. 2018, *ApJ*, 856, 40, doi: [10.3847/1538-4357/aaae8](https://doi.org/10.3847/1538-4357/aaae8)
- Matt, S. P., MacGregor, K. B., Pinsonneault, M. H., & Greene, T. P. 2012, *ApJL*, 754, L26, doi: [10.1088/2041-8205/754/2/L26](https://doi.org/10.1088/2041-8205/754/2/L26)
- McQuillan, A., Mazeh, T., & Aigrain, S. 2014, *ApJS*, 211, 24, doi: [10.1088/0067-0049/211/2/24](https://doi.org/10.1088/0067-0049/211/2/24)
- Meibom, S., Mathieu, R. D., & Stassun, K. G. 2007, *ApJL*, 665, L155, doi: [10.1086/521437](https://doi.org/10.1086/521437)
- Nakajima, T., & Morino, J.-I. 2012, *AJ*, 143, 2, doi: [10.1088/0004-6256/143/1/2](https://doi.org/10.1088/0004-6256/143/1/2)
- Nguyen, C. T., Costa, G., Girardi, L., et al. 2022, *A&A*, 665, A126, doi: [10.1051/0004-6361/202244166](https://doi.org/10.1051/0004-6361/202244166)
- Nielsen, M. B., Gizon, L., Schunker, H., & Karoff, C. 2013, *A&A*, 557, L10, doi: [10.1051/0004-6361/201321912](https://doi.org/10.1051/0004-6361/201321912)
- Nordström, B., Mayor, M., Andersen, J., et al. 2004, *A&A*, 418, 989, doi: [10.1051/0004-6361:20035959](https://doi.org/10.1051/0004-6361:20035959)
- Owocicki, S. P., Cranmer, S. R., & Blondin, J. M. 1994, *ApJ*, 424, 887, doi: [10.1086/173938](https://doi.org/10.1086/173938)
- Patience, J., Ghez, A. M., Reid, I. N., & Matthews, K. 2002, *AJ*, 123, 1570, doi: [10.1086/338431](https://doi.org/10.1086/338431)
- Pecaut, M. J., & Mamajek, E. E. 2013, *ApJS*, 208, 9, doi: [10.1088/0067-0049/208/1/9](https://doi.org/10.1088/0067-0049/208/1/9)
- Pereira, F., Grunblatt, S. K., Psaridi, A., et al. 2024, *MNRAS*, 527, 6332, doi: [10.1093/mnras/stad3449](https://doi.org/10.1093/mnras/stad3449)
- Perryman, M. A. C., Brown, A. G. A., Lebreton, Y., et al. 1998, *A&A*, 331, 81, doi: [10.48550/arXiv.astro-ph/9707253](https://doi.org/10.48550/arXiv.astro-ph/9707253)
- Phillips, A., Kochanek, C. S., Jayasinghe, T., et al. 2024, *MNRAS*, 527, 5588, doi: [10.1093/mnras/stad3564](https://doi.org/10.1093/mnras/stad3564)
- Pouilly, K., Bouvier, J., Alecian, E., et al. 2020, *A&A*, 642, A99, doi: [10.1051/0004-6361/202038086](https://doi.org/10.1051/0004-6361/202038086)
- Quinn, S. N., White, R. J., Latham, D. W., et al. 2012, *ApJL*, 756, L33, doi: [10.1088/2041-8205/756/2/L33](https://doi.org/10.1088/2041-8205/756/2/L33)
- Rampalli, R., Smock, A., Newton, E. R., Daniel, K. J., & Curtis, J. L. 2023, *ApJ*, 958, 76, doi: [10.3847/1538-4357/acff69](https://doi.org/10.3847/1538-4357/acff69)
- Reddy, B. E., Tomkin, J., Lambert, D. L., & Allende Prieto, C. 2003, *MNRAS*, 340, 304, doi: [10.1046/j.1365-8711.2003.06305.x](https://doi.org/10.1046/j.1365-8711.2003.06305.x)
- Reinhold, T., Shapiro, A. I., Solanki, S. K., & Basri, G. 2023, *A&A*, 678, A24, doi: [10.1051/0004-6361/202346789](https://doi.org/10.1051/0004-6361/202346789)

- Rice, M., Wang, S., & Laughlin, G. 2022, *ApJL*, 926, L17, doi: [10.3847/2041-8213/ac502d](https://doi.org/10.3847/2041-8213/ac502d)
- Ricker, G. R., Winn, J. N., Vanderspek, R., et al. 2014, in *Society of Photo-Optical Instrumentation Engineers (SPIE) Conference Series*, Vol. 9143, *Space Telescopes and Instrumentation 2014: Optical, Infrared, and Millimeter Wave*, ed. J. Oschmann, Jacobus M., M. Clampin, G. G. Fazio, & H. A. MacEwen, 914320, doi: [10.1117/12.2063489](https://doi.org/10.1117/12.2063489)
- Schatzman, E. 1962, *Annales d'Astrophysique*, 25, 18
- Schlaufman, K. C. 2010, *ApJ*, 719, 602, doi: [10.1088/0004-637X/719/1/602](https://doi.org/10.1088/0004-637X/719/1/602)
- Schröder, C., Reiners, A., & Schmitt, J. H. M. M. 2009, *A&A*, 493, 1099, doi: [10.1051/0004-6361:200810377](https://doi.org/10.1051/0004-6361:200810377)
- Spalding, C., & Winn, J. N. 2022, *ApJ*, 927, 22, doi: [10.3847/1538-4357/ac4993](https://doi.org/10.3847/1538-4357/ac4993)
- Taylor, B. J. 2006, *AJ*, 132, 2453, doi: [10.1086/508610](https://doi.org/10.1086/508610)
- Torres, G., Andersen, J., & Giménez, A. 2010, *A&A Rv*, 18, 67, doi: [10.1007/s00159-009-0025-1](https://doi.org/10.1007/s00159-009-0025-1)
- van Belle, G. T. 2012, *A&A Rv*, 20, 51, doi: [10.1007/s00159-012-0051-2](https://doi.org/10.1007/s00159-012-0051-2)
- van Saders, J. L., & Pinsonneault, M. H. 2013, *ApJ*, 776, 67, doi: [10.1088/0004-637X/776/2/67](https://doi.org/10.1088/0004-637X/776/2/67)
- van Saders, J. L., Pinsonneault, M. H., & Barbieri, M. 2019, *ApJ*, 872, 128, doi: [10.3847/1538-4357/aafafe](https://doi.org/10.3847/1538-4357/aafafe)
- Weber, E. J., & Davis, Leverett, J. 1967, *ApJ*, 148, 217, doi: [10.1086/149138](https://doi.org/10.1086/149138)
- Wilson, O. C., & Skumanich, A. 1964, *ApJ*, 140, 1401, doi: [10.1086/148046](https://doi.org/10.1086/148046)
- Winn, J. N., Fabrycky, D., Albrecht, S., & Johnson, J. A. 2010, *ApJL*, 718, L145, doi: [10.1088/2041-8205/718/2/L145](https://doi.org/10.1088/2041-8205/718/2/L145)
- Wolff, S., & Simon, T. 1997, *PASP*, 109, 759, doi: [10.1086/133942](https://doi.org/10.1086/133942)
- Wright, J., Rice, M., Wang, X.-Y., Hixenbaugh, K., & Wang, S. 2023, *AJ*, 166, 217, doi: [10.3847/1538-3881/ad0131](https://doi.org/10.3847/1538-3881/ad0131)
- Zahn, J. P., & Bouchet, L. 1989, *A&A*, 223, 112
- Zwintz, K., Neiner, C., Kochukhov, O., et al. 2020, *A&A*, 643, A110, doi: [10.1051/0004-6361/202038210](https://doi.org/10.1051/0004-6361/202038210)